Tribology Letters (2020) 68:127
https://doi.org/10.1007/s11249-020-01363-0

ORIGINAL PAPER

Tribological Analysis of Contacts Between Glass and Tungsten Carbide Near the Glass Transition Temperature

Petr Chizhik[1] · Marcel Friedrichs[2] · Dirk Dietzel[1,3] · André Schirmeisen[1,3]

Received: 10 June 2020 / Accepted: 19 October 2020 / Published online: 7 November 2020

Abstract

In recent years, the tribological contact between hard solids and glass at high temperatures has been identified as a crucial aspect in emerging technical applications like e.g., precision glass molding. To optimize such tribological systems, especially, the internal transformations of the glasses need to be considered, since these can determine which kind of energy dissipation channels become relevant, when the temperature of a glass is increasing and approaching the glass transition temperature. Here, we now introduce a new tribometer specifically developed for the analysis of glasses at elevated temperatures. Using this tribometer, we characterize friction of contacts between tungsten carbide (WC) and soda lime glass as a function of temperature, while additionally PMMA was analyzed for comparison. Our experiments reveal different tribological regimes where either simple sliding, surface fracturing, or surface deformation can be identified as relevant interface processes for the tribological behavior.

Graphical Abstract

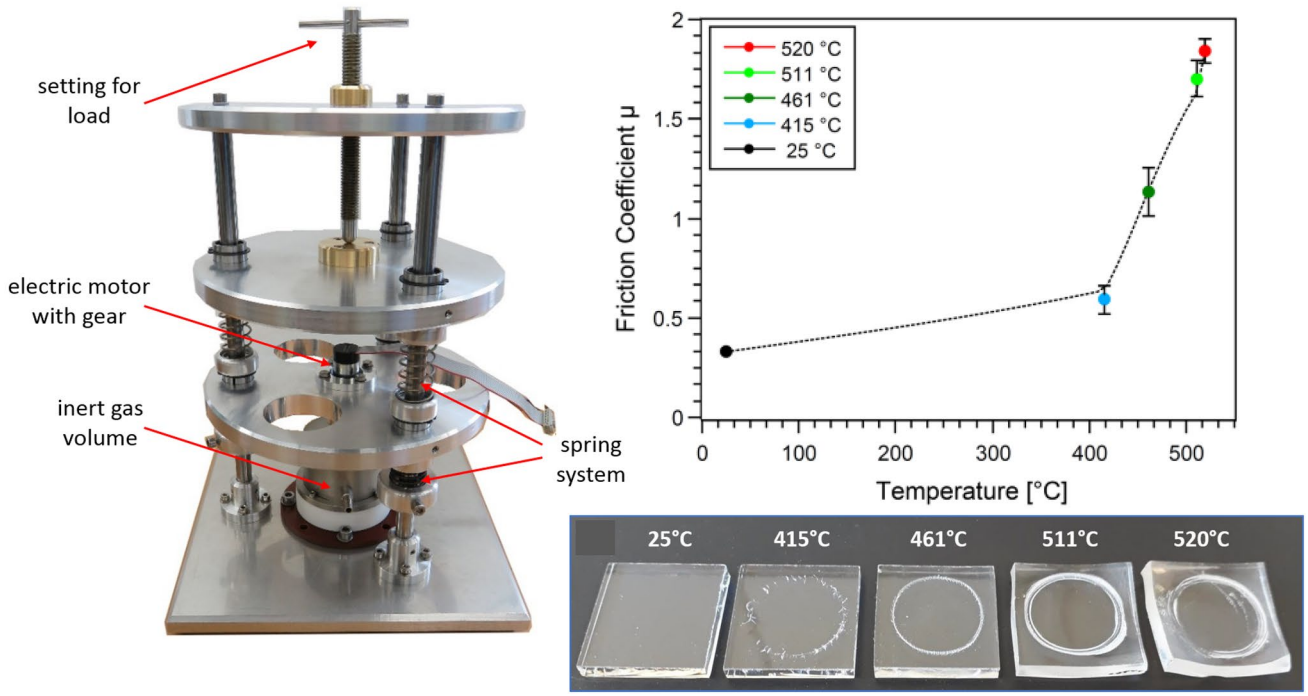

Keywords High-temperature tribometer · Soda lime glass · PMMA · Friction · Glass transition temperature

Extended author information available on the last page of the article

1 Introduction

Measuring friction of contacts formed between solids and glasses at temperatures close to the glass transition is a problem of both fundamental scientific interest and technological relevance. Concerning technological applications, understanding the tribological mechanisms is particularly relevant for precision glass molding (PGM) [1–4], where optical components are formed in a one-step process from heated glass by using molds made typically from tungsten carbide (WC) with a precisely machined and smooth surface. Since the production of the pressing tools, i.e., the molds, is an expensive and complex process, their lifetime ultimately determines the economic viability of the method.

To prevent friction and wear of the molds, different strategies like surface coating or optimization of process parameters can be applied. But in both cases, it is essential to understand the specific tribological system formed by the pressing tool and the heated glass in an increasingly rubbery state around the transition temperature. As a consequence, first high-temperature friction measurements between WC and glass have been performed using equipment, closely resembling the geometry used in PGM [5, 6].

From a more fundamental point of view, it is also interesting to systematically explore how the tribological properties of glasses are changing close to the glass transition temperature T_G. In principle, the internal processes of glasses upon temperature changes are relatively well known [7, 8] and a promising route to understand the tribological behavior lies in considering the obvious analogies to polymer systems. These materials have been extensively studied by techniques like e.g., dynamical mechanical analysis (DMA) [9–12] and the resulting temperature dependence of the elastic and viscoelastic behavior can be explained by internal relaxations of the polymers. The link between tribology and these internal relaxations becomes particularly clear in recent analysis by friction force microscopy which directly correlates the different temperature-dependent transitions within the polymers to characteristic energy barriers derived from nanoscale friction [13–18]. But already for macroscopic systems these mechanisms were anticipated based on experiments, which explored the influence of velocity and temperature on polymer friction [19]. Regarding the temperature dependence alone, friction is typically characterized by a significant increase around the glass transition temperature that can be related to the additional energy dissipation once the molecule relaxation processes result in an increasingly viscoelastic behavior of the material. Over a wider range of temperature, friction of polymers can then be separated into three parts: At low temperatures, the material behaves as an elastic solid with a constant friction coefficient. At higher temperatures, friction increases when T approaches T_G, before it finally decreases in the viscous regime above T_G [6, 20, 21]. However, transferring this concept to glasses is not entirely straightforward due to the differences of the materials. Most prominently, the entanglement of long polymeric chains cannot be compared directly to the behavior of the smaller molecules forming the glass, which nonetheless show a strong dependence of the mechanical properties on temperature [22–26].

Despite this motivation related to both fundamental and technological aspect, so far, there are only few systematic tribological studies of glasses at high temperatures. In principle, most current tribometers are optimized for the general analysis of friction and wear between hard surfaces close to room temperature either in dry or lubricated environments [27–33]. Nonetheless, high-temperature systems are also available, but they are rather applied to hard contacts between ceramics [34] or metallic materials, with the analysis of metallic glasses [35] or steel [36] as prominent examples. Tribological characterization of glasses at high temperatures has instead been based on compression tests [37–40] or was done by using tribometers specifically designed to mimick the PGM process [5]. In the latter case, a geometry was used where the glass sample is confined between flat metal surfaces in relative lateral movement, which allowed to analyze stick-slip-behavior of glass friction [41]. The potential to apply pin-on-disk configurations to the problem of high-temperature glass friction was highlighted only recently [42]. In this work, we will now present experiments using a novel high-temperature tribometer, that was constructed to study the general tribological properties of WC/glass contacts at temperatures up to 700 °C using a standard pin-on-disk configuration. Being home-build, the tribometer is very cost-efficient and the construction can easily be modified if required.

As a reference glass, we have chosen B270, which is a very common and well-known soda lime glass that is routinely used in a large variety of applications, among which is also precision glass molding. The material is readily available, relatively cheap, and all its core characteristics are well documented, with a glass transition temperature of 533 °C, an annealing temperature of 541 °C, a softening temperature T_S of 724 °C, and a young modulus at room temperature of 71.5 kN/mm^2. Most importantly, there was no adhesion of glass to the tungsten carbide pins at high temperatures. In addition, acrylic glass (polymethylmethacrylate, PMMA) was used as a complementary sample. Based on the experimental results for these two materials, we will then develop a first tribological model for the WC/glass contact, which considers different friction regimes related to sliding, crack formation, and plastic/viscoelastic deformation.

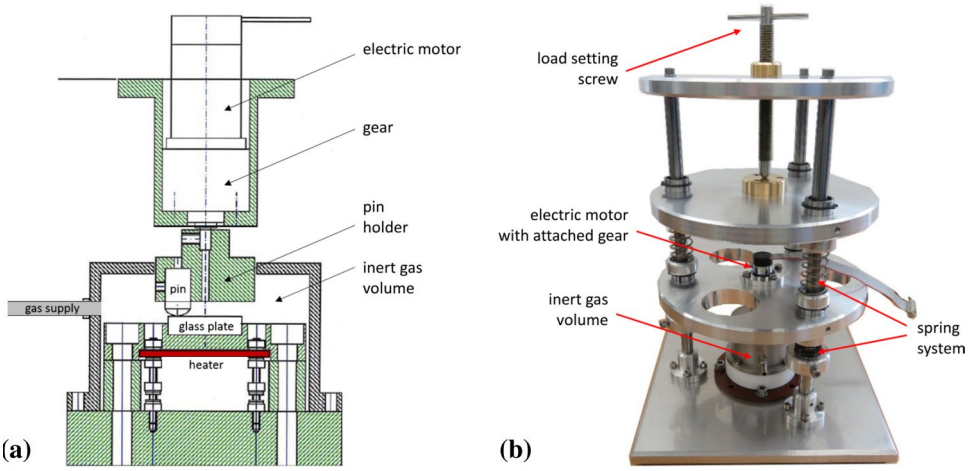

Fig. 1 **a** Schematic diagram of the high-temperature pin-on-disk tribometer. The lower part of the figure depicts a chamber containing an inert gas and which also houses both the tungsten carbide pin and the glass sample. The integrated heater, which is positioned directly underneath the metal glass holder, is shown in red. The upper part of the figure shows the electric motor with an attached gear. The motor directly drives the pin holder within the high-temperature chamber. A thermal insulation at the bottom of the gas volume ensures that the tribometer can be used as a tabletop device even during high-temperature operation. **b** Photograph of the high-temperature pin-on-disk tribometer with inert gas volume, electric motor with gear, and spring system for precise load setting

2 Experimental Set-up

In principle, the general construction of our new apparatus is based on a previously developed pin-on-disk tribometer, that was used for the analysis of oil lubricated friction and the characterization of oil additives [33]. As a main modification, the new design is now equipped with a heating chamber that allows to reach temperatures of up to 700 °C, thereby exceeding the glass transition temperatures T_G of typical materials used in precision glass molding like e.g., Schott B270 and Sumita K-VC89 with glass transition temperatures of 533 °C and 528 °C. Inside the chamber, heating is facilitated by a resistive pyrolithic boron nitride heater with a maximum input power of 220W (Tectra, HTR100135, size: 35 mm × 25 mm × 2 mm). In order to minimize mechanical strain related to thermal expansion at high temperatures, the heater is only loosely fixed at two opposite corners. For good thermal contact, the heater is positioned directly underneath a metal glass holder that is equipped with a cavity to fit the glass (see Fig. 1a). To enable tabletop operation of our tribometer and to minimize heat losses, both the boron nitride heater and the metallic glass holder are mounted on a ceramic base plate. Additionally, both components are enclosed by a cylindrical steel housing (Fig. 1).

To prevent oxidization within the heating chamber, the tribometer is operated in a protective gas environment. More specifically, the heating chamber is flooded by nitrogen through a small inlet at the side of the cylindrical steel housing (see Fig. 1a). A constant nitrogen flow of appr. 10 l/min is typically chosen, which results in the build-up of excess pressure within the heating chamber, that is released through a narrow opening on top formed between the heating chamber and the pin holder. This geometry also ensures, that the electrical motor, which facilitates force detection as well, is sufficiently separated from the heat source and remains unaffected from the elevated temperatures.

In this set-up, friction is then measured between the pins and the glass substrates. Throughout this work we have used uncoated pins made of cemented tungsten carbide with cobalt binder content below 1 wt%, that were provided by Aixtooling GmbH, Aachen, Germany. The pins are of 14 mm overall length with a tube diameter of 7 mm. The tube is capped by a section of a sphere with a radius of 6 mm, which is in contact with the glass during the experiments. The surface of this sphere is highly polished with a roughness R_a of only a few nm. The glass plates used in our experiments are of square shape with edge lengths of 20 mm and a thickness of 5 mm. Experiments have also been performed using thinner glas samples, but no apparent difference has been found. For each measurement presented in this work, a new glass substrate has been used. The tungsten carbide pins, on the other hand, proved to be largely unaffected by wear and could often be used several times. Both the pin and the glass substrate were cleaned using isopropanol before each measurement.

To perform the tribological analysis, the pins are rotated across the glass substrates in circular motion with a radius of 7.5 mm. The rotation is facilitated by an electrical motor with linearized characteristics (Maxxon A-max19). For this motor, the current required to maintain the rotational frequency is a direct measure for the

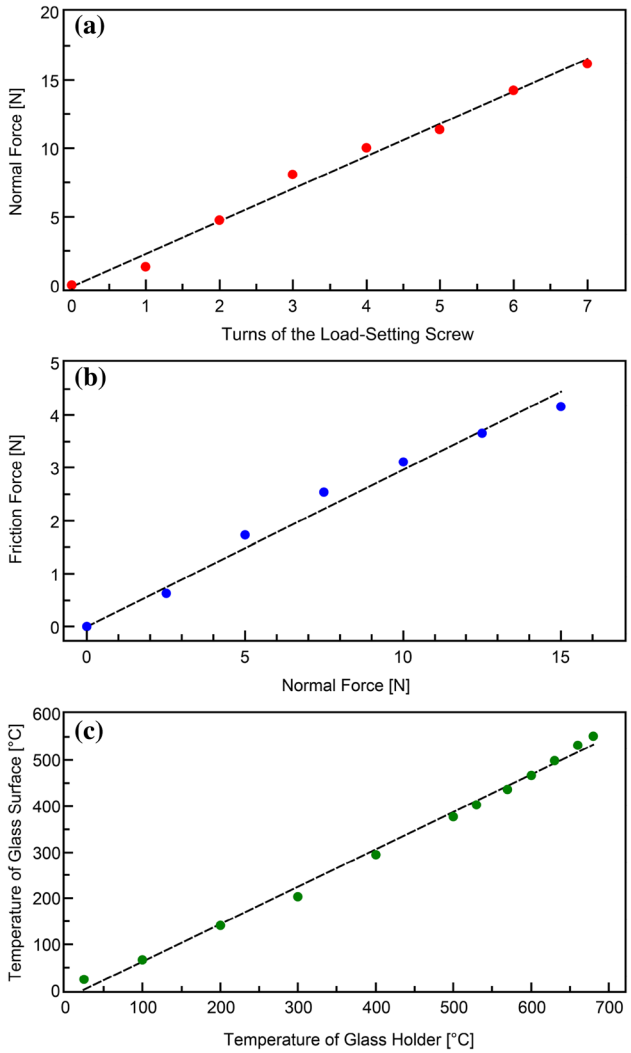

Fig. 2 Calibration of the high-temperature glass tribometer. **a** Characterization of the spring system for load setting. The normal force values show a linear dependence on the turns of the load setting screw as expected for springs operated in the elastic regime. **b** Friction force signal as a function of the normal load measured for B270 glass at room temperature. The recorded friction values can well be described by a linear increase (continuous line) in accordance to Amontons' law. **c** Temperature calibration curve recorded during continuous heating of the glass. The temperature measured at the glass surface (green spheres) is plotted versus the temperature of the glass holder that is recorded during tribological experiments. The resulting curve can well be approximated by a linear fit (continuous line)

torque generated by the interfacial friction between the pin and the glass. To mimic the conditions of precision glass molding, low sliding velocities in the range of mm/s are required. This is achieved by installing a gear reduction of 131:1, which reduces the typical rotation frequencies of a few 100 min^{-1} while still providing a sufficient sensitivity to friction changes. For all experiments shown in Sect. 3 rotational frequencies of 10 min^{-1} were chosen, which is equivalent to a sliding velocity of about 8 mm/s.

Additionally, the tribometer is equipped with a system of counteracting springs, where a load setting screw (see Fig. 1b) can be used to adjust the normal force acting on the pin/glass contact in a range from 0 to 20 N. The construction of the spring system, with springs above and beneath the ground plate carrying the electrical motor, ensures, that the overall load is zero once the pin comes into contact with the substrate. After that, operation of the load setting screw steadily compresses the springs resulting in a linear increase of the normal load by 2.3 N/rotation (see Fig. 2a). A rough estimation based on contact mechanical calculations for a metal sphere on a planar glass substrate at room temperature shows, that normal forces of only a few N are already equivalent to contact pressures of up to 1–2 GPa.

For a quantitative determination of friction forces, we have to take into account that for all experiments the friction signal always consists of two components: (i) sliding friction between the pin and glass substrate and (ii) the internal friction of the motor and gear. The second component is a constant and can be obtained as a reference level when rotating the pin attachment without contact between pin and plate. Only the difference between the total friction (i+ii) and the reference level (ii) then represents the sliding friction between pin and glass, which is the main result of all our tribometer experiments.

Considering this, also the dependence of the friction force on the normal load can be characterized. This was done at room temperature using a B270 glass substrate and a standard pin at a rotational speed of 10 min^{-1}. Our experiments show, that the friction force depends linearly on the normal force as expected based on Amontons' law. Absolute friction values have been obtained using calibration factors provided by the motor manufacturer under consideration of the gear reduction. Ultimately, a sliding friction coefficient of $\mu = 0.29$ is derived from the results shown in Fig. 2b.

To monitor the temperature during our experiments, a thermocouple is inserted into the metal glass holder. Due to the generally poor heat conduction of glass materials, the value registered by this thermocouple does not represent the surface temperature of the glass, which is additionally cooled by the nitrogen flow. Therefore, the actual surface temperature must be correlated for each type of glass to the temperature of the glass holder in a separate measurement. In most cases, the resulting temperature calibration curve can well be approximated by a linear fit as indicated in Fig. 2c for the case of a B270 glass.

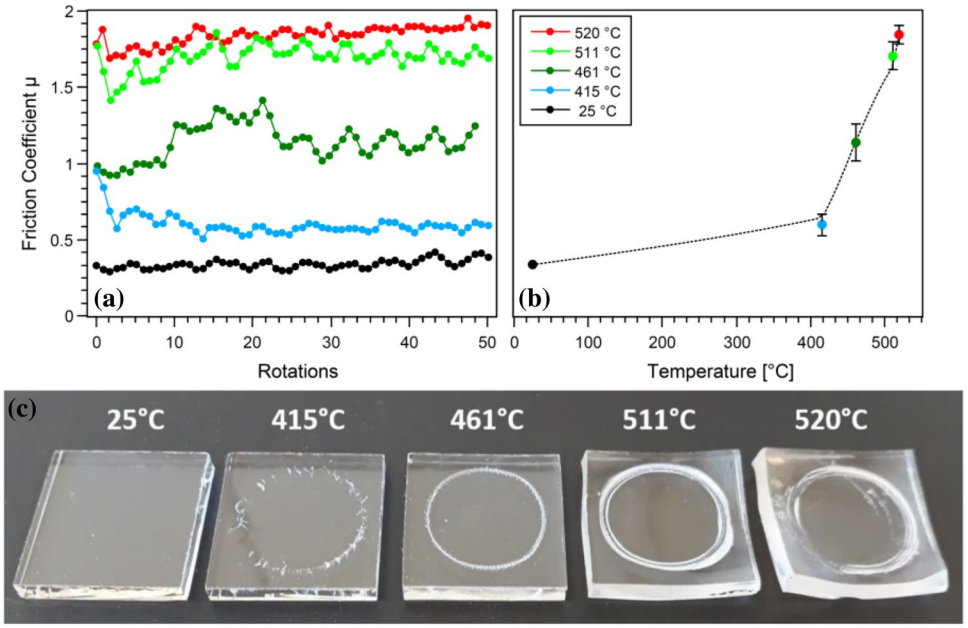

Fig. 3 Temperature dependent friction measurements on the glass B270. **a** Friction coefficient vs. number of rotations recorded at different temperatures with a rotational frequency of 10 min^{-1} and a normal force of 5 N. **b** Average friction coefficient extracted from **a** plotted versus the surface temperature of the glass. **c** Photographic images of the glass samples used in **a**

3 Experimental Results

To obtain the experimental data shown in the upcoming paragraphs, two systematic approaches have been used. In the first approach, friction is analyzed at constant temperature. Therefore, the glass is slowly heated up to the required temperature. Once this temperature has stabilized, the motor is started and the pin is brought into contact with the surface at a constant load, while the friction force signal is permanently recorded for a defined amount of time. To characterize the temperature dependence of the tribological properties, this procedure must be repeated for a sufficiently high number of temperatures in the relevant temperature range. Alternatively, a second approach can be used. In this case, the measurement is started well below the glass transition temperature with a constant normal force and sliding velocity. Throughout the course of the measurement, the temperature is then continuously increased until the maximum temperature is reached. Optionally, the measurement can be continued by slowly decreasing the temperature again. While the first approach is especially suitable for a precise characterization of the tribological properties at a fixed temperature, the second approach allows for a faster analysis of general trends in the temperature dependence. However, any modification of the sample system induced at an earlier stage of the temperature variation might potentially influence the results later on.

Based on the first approach, Fig. 3a shows the resulting friction vs. time curves for B270 glass obtained at 5 different temperatures, a rotational frequency of 10 min^{-1} and a normal load of 5N. The normal force and

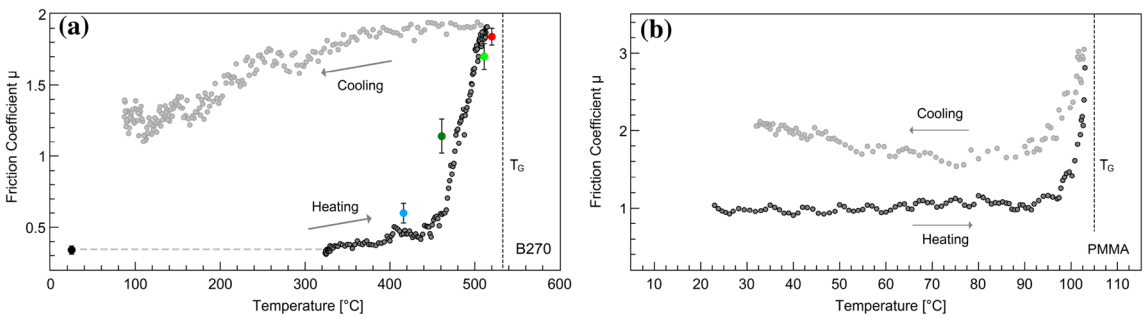

Fig. 4 Measurements of the friction coefficients on B270 glass (**a**) and PMMA (**b**) recorded during continuous temperature variation, i.e., heating and cooling (dark and light gray spheres). For comparison, the friction coefficients obtained for steady temperatures on B270 glass (see Fig. 3b) have been added to **a** as colored symbols. In both **a** and **b**, the vertical dashed line indicates the respective glass transition temperature T_G

the rotational velocity were chosen to ensure optimum operation of the tribometer while at the same time allowing to probe the effects related to the gradual softening of the glass. In Fig. 3a, the reference level of the motor current has already been subtracted and an effective friction coefficient was calculated from the resulting current signal. For all 5 temperatures, the WC pins used in the experiments did not show any discernible signs of wear or surface modification. Fig. 3b then displays the average friction coefficient as a function of temperature. We find, that the frcition coefficient is continuously increasing with temperature. At room temperature, we find a friction coefficient of $\mu = 0.34$, which is similar to the sliding friction coefficients for glass/WC contacts as reported in Ref. [6]. Finally, Fig. 3c contains images of the 5 glass samples after the tribological tests. The samples show distinct differences in the level of deformations, cracks and scratches. More specifically, the glass tested at room temperature is mostly unaffected by the experiment, while glasses analyzed at 415 °C and 461 °C show scratches in combination with cracks perpendicular to the direction of pin movement. For even higher temperatures, i.e., at 511 °C and 520 °C, we can observe significant deformations of the glass, that go along with more visible effects of wear along the circular area of contact.

To check, how the data points obtained at fixed temperature compare to measurements during which the temperature is continuously varied, we performed a second experiment on B270 glass using the same normal load and rotational speed as before. However, this time we continuously increased the temperature between $T_{start} = 323\,°C$ and $T_{end} = 515\,°C$ at a rate of appr. 20 °C per minute while the motor current was continuously recorded. The resulting friction data are shown in Fig. 4a (dark gray symbols). We find, that friction is almost independent of temperature well below the glass transition temperature. At around 460 °C friction starts to increase slowly. The friction vs. temperature curve then becomes increasingly steeper as the temperature approaches the glass transition. At the maximum temperature T_{end} friction has increased by approximately a factor of 6 compared to the starting temperature T_{start}.

For a direct comparison between the two sets of experiments (i.e., fixed vs. varying glass temperature), the friction coefficients obtained at fixed temperature have been added to Fig. 4a as colored symbols. We find that the two approaches yield very similar results. Therefore, cracks and surface modifications induced at lower temperatures do not seem to significantly alter the energy dissipation process later on.

In addition, the light gray symbols of Fig. 4a show the friction data recorded during the cooling process after the maximum temperature was reached. One might expect, that the friction coefficient should decrease as the temperature decreases. However, this is not the case. Instead, friction remains on an elevated level upon cooling. This behavior implies, that the irreversible changes induced to the glasses related to deformation of the sample and altered surface roughness do affect the friction coefficient significantly.

As a second material we also tested PMMA using the same approach of continuous temperature variation. Due to the drastically different glass transition temperature T_{G} of PMMA our temperature range was limited to $20\,°C < T < 103\,°C$, which is accessible without flushing the heating chamber with nitrogen. Above a temperature of approximately 105 °C meaningful experiments are no longer possible, since the material becomes too soft and interaction between the pin and the polymer does no longer resemble a defined sliding process.

The resulting friction coefficient as a function of temperature is shown in Fig. 4b, where friction was recorded during heating and cooling. Especially the heating branch (dark gray symbols) looks very similar to the previously described results for B270. We find, that the friction coefficient is constant in the low temperature range and only increases once the temperature exceeds 95 °C. Upon cooling (light gray symbols), friction decreases again and becomes relatively constant for temperatures below 90 °C, with a friction coefficient roughly 50% higher than during heating.

4 Discussion

So far, our results have revealed the distinct temperature dependence of friction and wear between tungsten carbide and glasses at elevated temperatures. In addition, there are numerous temperature dependent studies of non-tribological glass properties, which can help to understand the tribological processes in more detail. In particular, mechanical analysis of soda lime glass revealed a similar temperature dependence, where the elastic modulus remained relatively constant for a range of several 100 °C, before a sharp decrease of the elastic modulus was observed when approaching the glass transition temperature [23]. This similarity emphasizes the general link between the mechanical properties and the tribological behavior.

With respect to surface modifications, tests using sharp spherical tips with radii of approximately 75 µm have revealed, that normal forces of 0.5N are not yet sufficient to induce scratches in soda lime glass at room temperature [43]. Consequently, it is not surprising, that a relatively blunt and smoothly rounded pin as used in our experiments does not immediately damage the surface and friction remains on a constant and relatively low level. Only at higher temperatures, we have observed an increasing amount of cracks along the path of the pin. This behavior can be understood based on models, where a decreasing energy barrier for fracture can be overcome by the shear

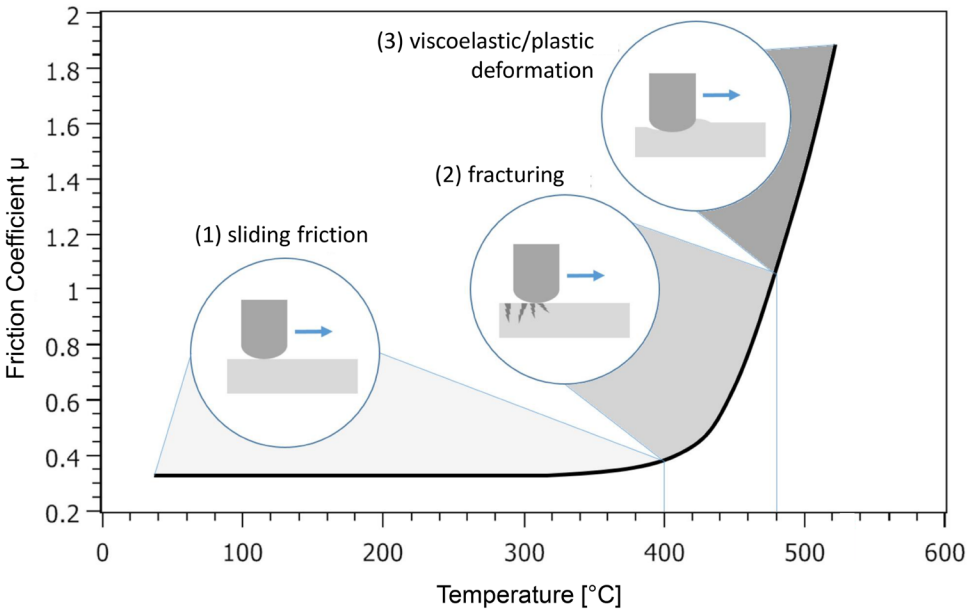

Fig. 5 Schematic representation of a typical friction coefficient vs. temperature curve on B270 glass obtained during heating. Three different regimes of pin-glass interaction are indicated

stress related to the sliding motion [44]. More specifically, in Fig. 4a, the elastic sliding friction regime with a constant friction coefficient extends up to a temperature of approximately 400 °C. For higher temperatures, albeit still significantly below the glass transition temperature, the subsequent increase of μ can then be linked to the formation of cracks during sliding. For $T = 415$ °C, the increase of the friction coefficient is still small, while only a limited number of cracks can be formed (see Fig. 3c). At higher temperatures (e.g., $T = 461$ °C in Fig. 3c), the friction coefficient increases with more cracks being formed in this thermally activated process. At even higher temperatures, the increase of the friction coefficient remains steep, when the glass is entering a regime, where effects related to increasing viscoelastic and plastic deformations of the glass can contribute to the energy dissipation process.

In summary, this suggests that our tribological experiments can be separated into 3 principle regimes, the general idea of which is illustrated in Fig. 5. Here, we distinguish (1) the sliding friction regime of an elastic solid, (2) the regime of crack formation, and (3) the temperature range, where viscoelastic and plastic deformation has to be considered as a potential factor for the energy dissipation process. However, the question remains how the different and potentially overlapping interface processes contribute to the friction signal. In each regime, either direct dissipation is possible via the channels described previously or an increased friction coefficient due to an overall increasing surface roughness and contact area in combination with increased wear. Furthermore, also temperature dependent adhesion between pins and the glass substrate can play a role, e.g., for the crack formation process [43].

Concerning the three regimes, it is noticable that the surface temperatures of Figs. 3 and 4a remain well below T_G, even when effects of the glass transition are supposed to have already set in. While this inconsistency might in part be related to general problems of using a pre-recorded temperature calibration curve, it also implies the relevance of higher subsurface temperatures related to temperature gradients between the metal holder and the glass surface.

Also our results on PMMA can well be reconciled with the material softening close to the glass transition temperature and the resulting contributions to friction by viscoelastic and plastic deformations as well as increased adhesion and contact area changes. Similar to the temperature dependence in our experiments, the mechanical analysis shows a relatively steep decrease of the elastic modulus within only a few °C before the glass transition temperature, an effect that can be mainly attributed to the α-transition of PMMA [45]. Although brittle behavior can be observed for PMMA under certain conditions [46], we did not notice any pronounced fracturing of the PMMA sample throughout our experiments and the temperature dependence fits well to the existing models [6, 20, 21] in the relevant temperature range.

When cooling the PMMA sample after the maximum temperature was reached, we find that the friction coefficient decreases immediately, but remains on an overall elevated level compared to the heating curve (see Fig. 4b). This effect can be rationalized, by considering reversible changes of the material properties in combination with irreversible modifications of the contact area, where an almost pointlike contact transformed into an extended contact area, with the pin now moving inside a groove formed during high-temperature testing. For the B270 glass, we observe a cooling behavior where the influence of previous temperatures and strain

becomes even more obvious. Down to a temperature of 350 °C, μ does not show any appreciable decrease but instead remains at the high-temperature limit. A straightforward hypothesis to explain this behavior would favor the irreversible changes of the contact geometry over the reversible changes within the material, a speculation, that might also explain, why Fig. 4a shows a strong similarity of μ for the two experimental approaches as long as the maximum temperature and thus the resulting contact areas are the same.

5 Conclusion

So far, our results have demonstrated how our newly developed high-temperature tribometer allows to analyze friction of tungsten carbide/glass interfaces at temperatures close to the glass transition. For the soda lime glass B270, we found that the friction coefficient remains at a relatively constant level for temperatures well below T_G, before a systematic increase of the friction coefficient is found. This increase was linked to different regimes of surface modifications including fracturing as well as plastic and viscoelastic deformation. In addition, similar regimes could be identified for PMMA, which was analyzed as a complementary material. Still, our pin-on-disk measurements do not yet allow to unambiguously separate direct effects of the different dissipation channels from the influence of contact area changes and adhesion. This problem seems to be linked to the irreversible friction changes that occur when cooling the glass after the maximum temperature was reached. In this context, measurements with varying maximum temperature might determine threshold temperatures for the hysteretic behavior. In addition, measuring the velocity dependence should be instructive, since both mechanical analysis and nanotribological AFM studies have highlighted the effects of strain rates on the internal dissipation [17, 18, 45]. Concerning PGM, such experiments are relevant, since they help to develop a basic understanding of tribological processes between molds and glass. Based on this knowledge, e.g., about the increase of friction as a function of temperature, the process parameters in PGM can then be optimized. In addition, a promising strategy for optimizing PGM molds lies in the use of protective coatings. Here, questions concerning the specific energy dissipation mechanisms are also relevant, e.g., to determine if rather hard or chemically inert coatings might be favorable for technical application. Moreover, initial tests of potential coatings can be performed in a quick and straightforward way using the simple pin-on-disk tribometer presented in this work, and promising candidates can then be tested in depth using real PGM machines.

Acknowledgements The author gratefully acknowledges the financial support of the Federal Ministry for Economic Affairs and Energy (BMWi) within the AiF/ZIM project 'InnoCoat' (ZF4266201HM6), DD thanks for financial support provided by the German Research Foundation (Project DI917/7-1)

Funding Open Access funding enabled and organized by Projekt DEAL.

Compliance with Ethical Standards

Conflict of interest The authors declare that they have no conflict of interest.

References

1. Zhang, L., Liu, W.: Precision glass molding: toward an optimal fabrication of optical lenses. Front. Mech. Eng. **12**(1), 3 (2017)
2. Zhou, T., Zhu, Z., Liu, X., Liang, Z., Wang, X.: A review of the precision glass molding of chalcogenide glass (ChG) for infrared optics. Micromachines **9**(7), 337 (2018)
3. Fischbach, K.D., Georgiadis, K., Wang, F., Dambon, O., Klocke, F., Chen, Y., Yi, A.Y.: Investigation of the effects of process parameters on the glass-to-mold sticking force during precision glass molding. Surf. Coat. Technol. **205**(2), 312 (2010)
4. Huang, C.Y., Hsiao, W.T., Huang, K.C., Chang, K.S., Chou, H.Y., Chou, C.P.: Fabrication of a double-sided micro-lens array by a glass molding technique. J. Micromech. Microeng. **21**(8), 085020 (2011)
5. Mosaddegh, P., Ziegert, J., Iqbal, W., Tohme, Y.: Apparatus for high temperature friction measurement. Precis. Eng. **35**(3), 473 (2011)
6. Mosaddegh, P., Ziegert, J.C.: Friction measurement in precision glass molding: an experimental study. J. Non-Cryst. Solids **357**(16–17), 3221 (2011)
7. Scholze, H.: Glass: Nature, Structure, and Properties. Springer, New York (1991)
8. Zarzycki, J.: Glasses and the Vitreous State. Cambridge University Press, Cambridge (1991)
9. Sgreccia, E., Chailan, J.F., Khadhraoui, M., Di Vona, M., Knauth, P.: Mechanical properties of proton-conducting sulfonated aromatic polymer membranes: stress strain tests and dynamical analysis. J. Power Sources **195**(23), 7770 (2010)
10. Martinez-Hernandez, A., Velasco-Santos, C., de Icaza, M., Castano, V.M.: Dynamical mechanical and thermal analysis of polymeric composites reinforced with keratin biofibers from chicken feathers. Composites Part B **38**(3), 405 (2007)
11. Deng, S., Hou, M., Ye, L.: Temperature-dependent elastic moduli of epoxies measured by DMA and their correlations to mechanical testing data. Polym. Test. **26**(6), 803 (2007)

12. Alves, N., Mano, J., Gomez Ribelles, J., Gomez Tejedor, J.: Departure from the Vogel behaviour in the glass transition—thermally stimulated recovery, creep and dynamic mechanical analysis studies. Polymer **45**(3), 1007 (2004)
13. Hammerschmidt, J.A., Moasser, B., Gladfelter, W.L., Haugstad, G., Jones, R.R.: Polymer viscoelastic properties measured by friction force microscopy. Macromolecules **29**(27), 8996 (1996)
14. Hammerschmidt, J.A., Gladfelter, W.L., Haugstad, G.: Probing polymer viscoelastic relaxations with temperature-controlled friction force microscopy. Macromolecules **32**(10), 3360 (1999)
15. Tocha, E., Schönherr, H., Vancso, G.J.: Surface relaxations of poly(methyl methacrylate) assessed by friction force microscopy on the nanoscale. Soft Matter **5**(7), 1489 (2009)
16. Sondhauss, J., Lantz, M., Gotsmann, B., Schirmeisen, A.: Beta-relaxation of PMMA: tip size and stress effects in friction force microscopy. Langmuir **31**(19), 5398 (2015)
17. Jansen, L., Schirmeisen, A., Hedrick, J.L., Lantz, M.A., Knoll, A., Cannara, R., Gotsmann, B.: Nanoscale frictional dissipation into shear-stressed polymer relaxations. Phys. Rev. Lett. **102**(23), 236101 (2009)
18. Jansen, L., Lantz, M.A., Knoll, A.W., Schirmeisen, A., Gotsmann, B.: Frictional dissipation in a polymer bilayer system. Langmuir **30**(6), 1557 (2014)
19. Mclaren, K.G., Tabor, D.: Visco-elastic properties and the friction of solids: friction of polymers : influence of speed and temperature. Nature **197**(4870), 856 (1963)
20. Bartenev, G.M., El'kin, A.I.: Nature and mechanism of friction of rubberlike polymers in different physical states. Polym. Mech. **3**(1), 85 (1967)
21. Bartenev, G.M., Lavrentev, V.V., Lee, L.H., Ludema, K.C.: Friction and wear of polymers. No. v. 6 in Tribology series. Elsevier Scientific Pub. Co.; Distributors for the U.S. and Canada, Elsevier/North-Holland, Amsterdam, New York (1981)
22. Marx, J.W., Sivertsen, J.M.: Temperature dependence of the elastic moduli and internal friction of silica and glass. J. Appl. Phys. **24**(1), 81 (1953)
23. McGRAW, D.A.: A method for determining Young's modulus of glass at elevated temperatures. J. Am. Ceram. Soc. **35**(1), 22 (1952)
24. Martendal, C.P., de Oliveira, A.P.N.: Glass viscosity at crystallization temperature: an approach. J. Therm. Anal. Calorim. **130**(3), 1903 (2017)
25. Shang, H., Rouxel, T., Buckley, M., Bernard, C.: Viscoelastic behavior of a soda-lime-silica glass in the 293–833 K range by micro-indentation. J. Mater. Res. **21**(3), 632 (2006)
26. Duffrene, L., Gy, R., Masnik, J.E., Kieffer, J., Bass, J.D.: Temperature dependence of the high-frequency viscoelastic behavior of a soda-lime-silica glass. J. Am. Ceram. Soc. **81**(5), 1278 (1998)
27. De Barros Bouchet, M.I., Martin, J.M., Avila, J., Kano, M., Yoshida, K., Tsuruda, T., Bai, S., Higuchi, Y., Ozawa, N., Kubo, M., Asensio, C.: Diamond-like carbon coating under oleic acid lubrication: evidence for graphene oxide formation in superlow friction. Sci. Rep. **7**(1), 1–13 (2017)
28. Berman, D., Erdemir, A., Sumant, A.V.: Few layer graphene to reduce wear and friction on sliding steel surfaces. Carbon **54**, 454 (2013)
29. Huang, G., Yu, Q., Ma, Z., Cai, M., Zhou, F., Liu, W.: Fluorinated candle soot as the lubricant additive of perfluoropolyether. Tribol. Lett. **65**(1), 28 (2017)
30. Xu, Y., Gao, F., Zhang, B., Nan, F., Xu, B.S.: Technology of self-repairing and reinforcement of metal worn surface. Adv. Manuf. **1**(1), 102 (2013)
31. Straffelini, G., Verlinski, S., Verma, P.C., Valota, G., Gialanella, S.: Wear and contact temperature evolution in pin-on-disc tribotesting of low-metallic friction material sliding against pearlitic cast iron. Tribol. Lett. **62**(3), 36 (2016)
32. Majdoub, F., Martin, J.M., Belin, M., Perret-Liaudet, J., Iovine, R.: Effect of temperature on lubricated steel/steel systems with or without fatty acids additives using an oscillating dynamic tribometer. Tribol. Lett. **54**(2), 171 (2014)
33. Chizhik, P., Dietzel, D., Bill, S., Schirmeisen, A.: Tribological properties of a phyllosilicate based microparticle oil additive. Wear **426–427**, 835 (2019)
34. Woydt, M., Habig, K.H.: High temperature tribology of ceramics. Tribol. Int. **22**(2), 75 (1989)
35. Segu, D.Z., Choi, J.H., Kim, S.S.: Sliding wear behavior of Fe-based bulk metallic glass at high temperature. J. Mech. Sci. Technol. **26**(11), 3565 (2012)
36. Varga, M., Flasch, M., Badisch, E.: Introduction of a novel tribometer especially designed for scratch, adhesion and hardness investigation up to 1000C. Proc. Inst. Mech. Eng. Part J **231**(4), 469 (2017)
37. Zhou, J., He, P., Yu, J., Lee, L.J., Shen, L., Yi, A.Y.: Investigation on the friction coefficient between graphene-coated silicon and glass using barrel compression test. J. Vacuum Sci. Technol. B **33**(3), 031213 (2015). https://doi.org/10.1116/1.4919769
38. Pallicity, T.D., Vu, A.T., Ramesh, K., Mahajan, P., Liu, G., Dambon, O.: Birefringence measurement for validation of simulation of precision glass molding process. J. Am. Ceram. Soc. **100**(10), 4680 (2017). https://doi.org/10.1111/jace.15010.
39. Trabelssi, M., Joseph, P.F.: Ring compression test for high-temperature glass using the generalized Navier law. J. Am. Ceram. Soc. **97**(10), 3257 (2014). https://doi.org/10.1111/jace.13138
40. Ananthasayanam, B., Joshi, D., Stairiker, M., Tardiff, M., Richardson, K.C., Joseph, P.F.: High temperature friction characterization for viscoelastic glass contacting a mold. J. Non-Cryst. Solids **385**, 100 (2014). https://doi.org/10.1016/j.jnoncrysol.2013.11.007.
41. P. Mosaddegh, J. Ziegert, The effect of temperature on the stick-slip friction behavior of optical glasses in precision glass molding. In: Applied Mechanics and Materials, vol 307, p. 381 (2013). https://doi.org/10.4028/www.scientific.net/AMM.307.381. Conference Name: Mechatronics and Computational Mechanics ISBN: 9783037856598 ISSN: 1662-7482, pp. 381–386 Publisher: Trans Tech Publications Ltd Volume: 307
42. Mosaddegh, P., Akbarzadeh, S., Zareei, M., Reiszadeh, H.: Tribological behavior of BK7 optical glass at elevated temperatures. Proc. Inst. Mech. Eng. Part J **233**(4), 580 (2018). https://doi.org/10.1177/1350650118788756
43. Li, K., Shapiro, Y., Li, J.: Scratch test of soda-lime glass. Acta Mater. **46**(15), 5569 (1998)
44. Wiederhorn, S.M.: Fracture surface energy of glass. J. Am. Ceram. Soc. **52**(2), 99 (1969)
45. Mulliken, A.D., Boyce, M.C.: Mechanics of the rate-dependent elastic plastic deformation of glassy polymers from low to high strain rates. Int. J. Solids Struct. **43**(5), 1331 (2006)
46. Matsushige, K., Radcliffe, S.V., Baer, E.: The pressure and temperature effects on brittle-to-ductile transition in PS and PMMA. J. Appl. Polym. Sci. **20**(7), 1853 (1976)

Affiliations

Petr Chizhik[1] · Marcel Friedrichs[2] · Dirk Dietzel[1,3] · André Schirmeisen[1,3]

✉ Dirk Dietzel
Dirk.dietzel@ap.physik.uni-giessen.de

André Schirmeisen
andre.schirmeisen@ap.physik.uni-giessen.de

[1] Institute of Applied Physics, Justus-Liebig-Univerity Giessen, Heinrich-Buff-Ring 16, 35392 Giessen, Germany

[2] Fraunhofer Institute for Production Technology IPT, Steinbachstrasse 17, 52074 Aachen, Germany

[3] TransMIT GmbH, Center for Adaptive, Cryotechnology and Sensors, Heinrich-Buff-Ring 16, 35392 Giessen, Germany